


Electric Circuit Model Analogy for Equilibrium Lattice Relaxation in Semiconductor Heterostructures

TEDI KUJOFSA ^{1,2} and JOHN E. AYERS¹

1.—Electrical and Computer Engineering Department, University of Connecticut, 371 Fairfield Way, Unit 4157, Storrs, CT 06269-4157, USA. 2.—e-mail: Tedi.Kujofsa@gmail.com

The design and analysis of semiconductor strained-layer device structures require an understanding of the equilibrium profiles of strain and dislocations associated with mismatched epitaxy. Although it has been shown that the equilibrium configuration for a general semiconductor strained-layer structure may be found numerically by energy minimization using an appropriate partitioning of the structure into sublayers, such an approach is computationally intense and non-intuitive. We have therefore developed a simple electric circuit model approach for the equilibrium analysis of these structures. In it, each sublayer of an epitaxial stack may be represented by an analogous circuit configuration involving an independent current source, a resistor, an independent voltage source, and an ideal diode. A multilayered structure may be built up by the connection of the appropriate number of these building blocks, and the node voltages in the analogous electric circuit correspond to the equilibrium strains in the original epitaxial structure. This enables analysis using widely accessible circuit simulators, and an intuitive understanding of electric circuits can easily be extended to the relaxation of strained-layer structures. Furthermore, the electrical circuit model may be extended to continuously-graded epitaxial layers by considering the limit as the individual sublayer thicknesses are diminished to zero. In this paper, we describe the mathematical foundation of the electrical circuit model, demonstrate its application to several representative structures involving $\text{In}_x\text{Ga}_{1-x}\text{As}$ strained layers on GaAs (001) substrates, and develop its extension to continuously-graded layers. This extension allows the development of analytical expressions for the strain, misfit dislocation density, critical layer thickness and widths of misfit dislocation free zones for a continuously-graded layer having an arbitrary compositional profile. It is similar to the transition from circuit theory, using lumped circuit elements, to electromagnetics, using distributed electrical quantities. We show this development using first principles, but, in a more general sense, Maxwell's equations of electromagnetics could be applied.

Key words: Electrical circuit model, relaxation, equilibrium in-plane strain, multilayers, compositionally-graded, InGaAs, GaAs

INTRODUCTION

The understanding of the equilibrium lattice relaxation has important implications in the

determination of the stability criteria for electronic and optical devices.^{1–6} Furthermore, the equilibrium configuration serves as the starting point for kinetically-limited lattice relaxation calculations and is critical in determining the effective stress and therefore the driving force for dislocation flow. Several models have been developed for the

(Received March 16, 2017; accepted August 16, 2017; published online September 13, 2017)

determination of the equilibrium configuration^{7–15} and, although it has been shown that the equilibrium configuration for a general semiconductor strained-layer structure may be determined numerically by energy minimization using an appropriate partitioning of the structure into sublayers,^{7–11} such an approach uses specialized code, is computationally intense, and does not lend itself to an intuitive understanding necessary for innovative structure design.

To avoid these limitations, and to enable the development of analytical solutions for compositionally-graded heterostructures, we propose the use of an electrical circuit model analogy. Several mechanical–electrical analogs have been developed and used, particularly for load beam analysis. The most common of these are the so-called “force-current” and “force-voltage” analogs,^{16–20} but others have also been developed. It is possible to use any of these to provide a physically correct description of behavior in a mechanical system; however, some are better suited to certain applications. For example, our work relates to the static behavior of a semiconductor heterostructure in equilibrium, and there is no need to include electrical components such as capacitors and inductors, which may be included for transient (time-dependent) modeling.

Among the previously published work on mechanical–electrical analogies, a report of particular interest is that by Olsson and Bath,²⁰ which describes two particular choices of analogies for application to problems of geophysics. Their second transcriptive system considers electrical current to be analogous to mechanical stress, electrical voltage to be analogous to mechanical strain, and electrical resistance to be analogous to the reciprocal of an elastic modulus. Olsson and Bath point out that an advantage of this transcriptive system is that it facilitates simple electrical analogies, and lends itself to series or parallel connections, which correspond to each other in the mechanical and electrical domains.

The purpose for developing an analogy between one field of physics and another is to take advantage of theoretical framework, which exists in one field but not the other. In a recent short publication,²¹ we have shown that an arbitrary semiconductor heterostructure, approximated by a stack of uniform composition layers, may be modeled using an electric circuit analogy similar to Olsson and Bath’s, in which electrical voltage is considered analogous to mechanical strain. In this model, each sublayer of a general strained-layer device may be represented by an analogous electrical circuit configuration involving an independent current source, a resistor, an independent voltage source, and an ideal diode. A multilayered structure may be built up by the connection of the appropriate number of these basic building blocks, after which the node voltages in the electric circuit correspond to the equilibrium strains in the original epitaxial structure. If any sublayer in

the structure is grown coherently on the sublayer below, the difference in strain in these sublayers is given by the lattice mismatch difference. This is modeled by introducing an independent voltage source between the nodes representing the two sublayers, and the resulting strains are analogous to the node voltages, which may be found using supernode theory. The theoretical framework of supernodes exists in electrical circuits but not in mechanical systems, and represents an important motivation for using the electric circuit analogy in this case. Another significant point is that the voltage source, which is related to the coherency state of the sublayer, is connected through an ideal diode, which conducts only in the case of coherent growth. Use of this device in the electric circuit analogy allows a physically correct description of the mechanical behavior, though no such device exists in mechanical systems. This represents a second key motivation for the application of the electric circuit model analogy to a strained semiconductor heterostructure.

Whereas, in the short paper,²¹ we only considered structures which were approximated by a stack of uniform layers, here, in the full-length paper, we show the application of the electrical circuit model approach to continuously-graded structures, wherein the strain is a continuous function of distance from the interface. This enables the development of a closed-form expression for the strain as a function of distance in a continuously-graded layer with any arbitrary compositional profile, including linear, exponential, power-law, or complementary error function profiles. This in turn allows an analytical solution for the critical layer thickness, widths of misfit dislocation free zones, and misfit dislocation density in these graded structures. In the present paper, we further develop the mathematical framework for the electrical circuit model approach, starting with a single strained layer and then generalizing to a multilayer structure. We relate the physical quantities in the epitaxial stack to those in an analogous electrical circuit. The electrical circuit model developed in this work is applicable for the determination of the equilibrium in-plane strain in any epitaxial material system. However, for application to crystals outside the diamond and zinc blende classes of materials, it will be necessary to modify the geometric factors related to the elastic properties and dislocation geometry. Here, we confine our discussion to zinc blende materials, and demonstrate the equilibrium analysis of a number of $\text{In}_x\text{Ga}_{1-x}\text{As}/\text{GaAs}$ (001) epitaxial structures, including a single strained layer, three-layer stacks, step-graded layers, linearly-graded layers and S-graded layers. We show that the strain results of the circuit model calculations are in agreement with the theory of Matthews and Blakeslee¹² for the single strained layer. We also develop exact results for the case of a linearly graded layer, whereas previously only an

approximate solution had been developed by Tersoff.^{13,14} In the approximate solution of Tersoff, it was assumed that the strain was completely relieved in the region containing dislocations, and that the dislocation line energy was independent of distance from the surface. We have not relied on these simplifying assumptions when applying the circuit model, and therefore provide exact in-plane strain results for the linearly-graded case. Furthermore, we show the extension of the circuit model to any continuously-graded semiconductor layer by taking the limit as the thickness of the individual sublayers approaches zero. This enables the development of analytical expressions for the strain, misfit dislocation density, critical layer thickness and widths of misfit dislocation free zones (MDFZ) in a continuously-graded epitaxial layer having any compositional grading profile, including linear,²² exponential,²³ power law, and S-graded^{9,24} profiles. The extension from a finite number of sublayers to the continuously-graded case is analogous to the transition from circuit theory, using lumped circuit elements, to electromagnetics, wherein the electrical quantities are distributed. We show the development of these expressions based on first principles, but, in a more general sense, Maxwell's equations of electromagnetics could be applied to continuously-graded strained layers.

PHYSICAL MODEL FOR EQUILIBRIUM STRAIN RELAXATION

Matthews and Blakeslee¹² developed a force-balance model for the equilibrium strain in a single layer with uniform composition. In it, the equilibrium strain was considered to be the value at which the glide force on a grown-in dislocation is equal to the opposing line tension. It has been shown that an equivalent result may be found by minimizing the sum of the strain energy and the line energy of misfit dislocations.¹⁵ In a partly-relaxed and compositionally uniform epitaxial layer (as shown in Fig. 1a) which contains misfit dislocations, the in-plane strain ε is given by

$$\varepsilon = f - \frac{f}{|f|} \rho b \sin \alpha \sin \phi, \quad (1)$$

where f is the lattice mismatch, $f \equiv (a_s - a_e)/a_e$, a_s and a_e are the relaxed lattice constants of the substrate and epitaxial crystal (cm), respectively, the term $f/|f|$ accounts for the sign of the mismatch, ρ is the linear misfit dislocation density in at the mismatched interface (cm^{-1}), b is the length of the Burgers vector (cm), α is the angle between the Burgers vector and dislocation line vector, and ϕ is the angle between the glide plane and interface. We will define the lattice mismatch of the substrate (layer 0) as $f_0 \equiv 0$ to simplify the mathematical descriptions that will follow. The areal strain energy

(erg/cm^2) associated with a partially-relaxed epitaxial layer with thickness h and an in-plane strain ε , is

$$E_\varepsilon = Yh\varepsilon^2, \quad (2)$$

where Y is the biaxial modulus (dyn/cm^2), $Y = C_{11} + C_{12} - 2C_{12}^2/C_{11} = 2G(1+\nu)/(1-\nu)$, G is the shear modulus (dyn/cm^2), C_{11} and C_{12} are the elastic stiffness constants (dyn/cm^2), and ν is the Poisson ratio (unitless). The line energy of dislocations per unit area (erg/cm^2), assuming two orthogonal networks with equal cross-sectional density, is

$$\begin{aligned} E_d &= \rho \frac{Gb^2(1-\nu \cos^2 \alpha)}{2\pi(1-\nu)} \left[\ln \left(\frac{h}{b} \right) + 1 \right] \\ &= (f - \varepsilon) \frac{f}{|f|} \frac{Gb(1-\nu \cos^2 \alpha)}{2\pi(1-\nu) \sin \alpha \sin \phi} \left[\ln \left(\frac{h}{b} \right) + 1 \right], \end{aligned} \quad (3)$$

Here, the dislocation energy is determined using a mean-field approach without including dislocation-dislocation interactions, and this is the main approximation used in this work. The equilibrium condition is found by minimizing the sum of the dislocation line energy and the strain energy, $E = E_d + E_\varepsilon$. Differentiating the energy, E , and setting the partial derivative to zero we obtain

$$\begin{aligned} \frac{\partial E}{\partial \varepsilon} &= \frac{\partial (E_\varepsilon + E_d)}{\partial \varepsilon} \\ &= 2Yh\varepsilon - \frac{f}{|f|} \frac{Gb(1-\nu \cos^2 \theta)}{2\pi(1-\nu) \sin \alpha \sin \phi} \left[\ln \left(\frac{h}{b} \right) + 1 \right] = 0. \end{aligned} \quad (4)$$

The solution for equilibrium in-plane strain, accounting for the possibility of pseudomorphic growth, is

$$\varepsilon(h) = \begin{cases} f, & h \leq h_c \\ \frac{f}{|f|} \frac{b(1-\nu \cos^2 \alpha)}{8\pi h(1+\nu) \sin \alpha \sin \phi} \left[\ln \left(\frac{h}{b} \right) + 1 \right], & h > h_c \end{cases}, \quad (5)$$

where h_c is the critical layer thickness at which it becomes energetically favorable to introduce misfit dislocations. Below h_c , the in-plane strain is equal to the coherency strain (lattice mismatch).

If we consider an epitaxial structure involving a stack of three disparate layers as shown in Fig. 1b, the strain in each layer may be related to the misfit dislocation densities for that layer and those below it. The in-plane strain ε_n in the n th sublayer of a general structure is given by

$$\varepsilon_n = f_n - \frac{f_n - f_{n-1}}{|f_n - f_{n-1}|} \sum_{j=1}^n \rho_j b_j \sin \alpha \sin \phi. \quad (6)$$

For the case of three layers illustrated in Fig. 1b, the in-plane strains are

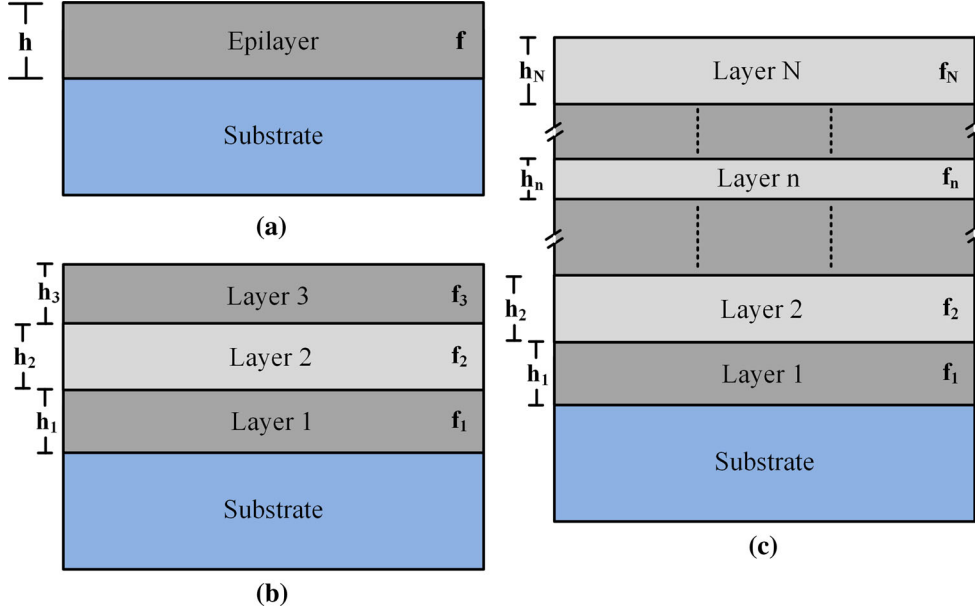


Fig. 1. Schematic representation of (a) a single compositionally uniform epitaxial layer with lattice mismatch f and thickness h , (b) an epitaxial structure comprised of three compositionally uniform layers with varying thickness and compositional mismatches and (c) a generalized epitaxial structure divided into N sublayers with varying thickness and mismatch.

$$\begin{aligned}
 \varepsilon_3 &= f_3 - \rho_3 b_3 \sin \alpha \sin \phi - \rho_2 b_2 \sin \alpha \sin \phi \\
 &\quad - \rho_1 b_1 \sin \alpha \sin \phi \\
 \varepsilon_2 &= f_2 - \rho_2 b_2 \sin \alpha \sin \phi - \rho_1 b_1 \sin \alpha \sin \phi \\
 \varepsilon_1 &= f_1 - \rho_1 b_1 \sin \alpha \sin \phi.
 \end{aligned} \tag{7}$$

By rearranging the equations above, the linear misfit dislocation densities for the three mismatched interfaces are given as

$$\begin{aligned}
 \rho_3 &= \frac{f_3 - f_2}{|f_3 - f_2|} \frac{(f_3 - \varepsilon_3) - (f_2 - \varepsilon_2)}{b_3 \sin \alpha \sin \phi} \\
 \rho_2 &= \frac{f_2 - f_1}{|f_2 - f_1|} \frac{(f_2 - \varepsilon_2) - (f_1 - \varepsilon_1)}{b_2 \sin \alpha \sin \phi} \\
 \rho_1 &= \frac{f_1 - f_0}{|f_1 - f_0|} \frac{f_1 - \varepsilon_1}{b_1 \sin \alpha \sin \phi}
 \end{aligned} \tag{8}$$

The sum of the strain and dislocation line energy per unit area may be found by adding the contributions of the three sublayers:

$$\begin{aligned}
 E &= E_{d,1} + E_{\varepsilon,1} + E_{d,2} + E_{\varepsilon,2} + E_{d,3} + E_{\varepsilon,3} \\
 &= \left[\begin{aligned}
 &\rho_1 \frac{G_1 b_1^2 (1 - \nu_1 \cos^2 \alpha)}{2\pi(1 - \nu_1)} \left[\ln \left(\frac{h_1 + h_2 + h_3}{b_1} \right) + 1 \right] + 2Y_1 h_1 \varepsilon_1 \\
 &+ \rho_2 \frac{G_2 b_2^2 (1 - \nu_2 \cos^2 \alpha)}{2\pi(1 - \nu_2)} \left[\ln \left(\frac{h_2 + h_3}{b_2} \right) + 1 \right] + 2Y_2 h_2 \varepsilon_2 \\
 &+ \rho_3 \frac{G_3 b_3^2 (1 - \nu_3 \cos^2 \alpha)}{2\pi(1 - \nu_3)} \left[\ln \left(\frac{h_3}{b_3} \right) + 1 \right] + 2Y_3 h_3 \varepsilon_3
 \end{aligned} \right].
 \end{aligned} \tag{9}$$

To determine the equilibrium strain of the three-sublayer system shown in Fig. 1b, we must differentiate the energy with respect to the in-plane strain at each sublayer and set each partial derivative equal to zero:

$$\begin{aligned}
 0 &= \frac{\partial E}{\partial \varepsilon_3} = 2Y_3 h_3 \varepsilon_3 - \frac{f_3 - f_2}{|f_3 - f_2|} \frac{G_3 b_3 (1 - \nu_3 \cos^2 \alpha)}{2\pi(1 - \nu_3) \sin \alpha \sin \phi} \left[\ln \left(\frac{h_3}{b_3} \right) + 1 \right] \\
 0 &= \frac{\partial E}{\partial \varepsilon_2} = 2Y_2 h_2 \varepsilon_2 - \frac{f_2 - f_1}{|f_2 - f_1|} \frac{G_2 b_2 (1 - \nu_2 \cos^2 \alpha)}{2\pi(1 - \nu_2) \sin \alpha \sin \phi} \left[\ln \left(\frac{h_2 + h_3}{b_2} \right) + 1 \right] \\
 &\quad + \frac{f_3 - f_2}{|f_3 - f_2|} \frac{G_3 b_3 (1 - \nu_3 \cos^2 \alpha)}{2\pi(1 - \nu_3) \sin \alpha \sin \phi} \left[\ln \left(\frac{h_3}{b_3} \right) + 1 \right] \\
 0 &= \frac{\partial E}{\partial \varepsilon_1} = 2Y_1 h_1 \varepsilon_1 - \frac{f_1 - f_0}{|f_1 - f_0|} \frac{G_1 b_1 (1 - \nu_1 \cos^2 \alpha)}{2\pi(1 - \nu_1) \sin \alpha \sin \phi} \left[\ln \left(\frac{h_1 + h_2 + h_3}{b_1} \right) + 1 \right] \\
 &\quad + \frac{f_2 - f_1}{|f_2 - f_1|} \frac{G_2 b_2 (1 - \nu_2 \cos^2 \alpha)}{2\pi(1 - \nu_2) \sin \alpha \sin \phi} \left[\ln \left(\frac{h_2 + h_3}{b_2} \right) + 1 \right].
 \end{aligned} \tag{10}$$

Concurrent solution of the three equations above yields the equilibrium in-plane strains ε_1 , ε_2 , and ε_3 . A similar analysis may be extended to any multilayered and compositionally-graded structure with N sublayers (as shown in Fig. 1c) and, in the general case, we consider the sum of the strain and dislocation line energy, $E = \sum_{j=1}^N E_{d,j} + E_{\varepsilon,j}$. The equilibrium in-plane strains are found by setting each partial derivative to zero, $\partial E / \partial \varepsilon_n = 0$ and solving the resulting system of N equations:

$$0 = \frac{\partial E}{\partial \varepsilon_N} = 2Y_N h_N \varepsilon_N - \frac{f_N - f_{N-1}}{|f_N - f_{N-1}|} \frac{G_N b_N (1 - \nu_N \cos^2 \alpha)}{2\pi(1 - \nu_N) \sin \alpha \sin \phi} \left[\ln \left(\frac{h_N}{b_N} \right) + 1 \right], \quad n = N$$

$$0 = \frac{\partial E}{\partial \varepsilon_n} = \left(\begin{array}{l} 2Y_n h_n \varepsilon_n - \frac{f_n - f_{n-1}}{|f_n - f_{n-1}|} \frac{G_n b_n (1 - \nu_n \cos^2 \alpha)}{2\pi(1 - \nu_n) \sin \alpha \sin \phi} \left[\ln \left(\sum_{j=n}^N \frac{h_j}{b_n} \right) + 1 \right] \\ + \frac{f_{n+1} - f_n}{|f_{n+1} - f_n|} \frac{G_{n+1} b_{n+1} (1 - \nu_{n+1} \cos^2 \alpha)}{2\pi(1 - \nu_{n+1}) \sin \alpha \sin \phi} \left[\ln \left(\sum_{j=n+1}^N \frac{h_j}{b_{n+1}} \right) + 1 \right] \end{array} \right), \quad 1 \leq n < N. \quad (11)$$

Essentially, the analysis provided above is the basis for the development of the Bertoli et al.⁷ model, which utilizes an *ad hoc* numerical approach to minimize the sum of the strain energy and dislocation line energy for an arbitrary multilayered heterostructure. The approach is generally applicable, and compositionally-

graded layers may be represented by staircase profiles with arbitrary precision.

ELECTRICAL CIRCUIT MODEL FOR EQUILIBRIUM STRAIN RELAXATION

The development of an electric circuit model stems from the fact that Eq. 4 resembles the node

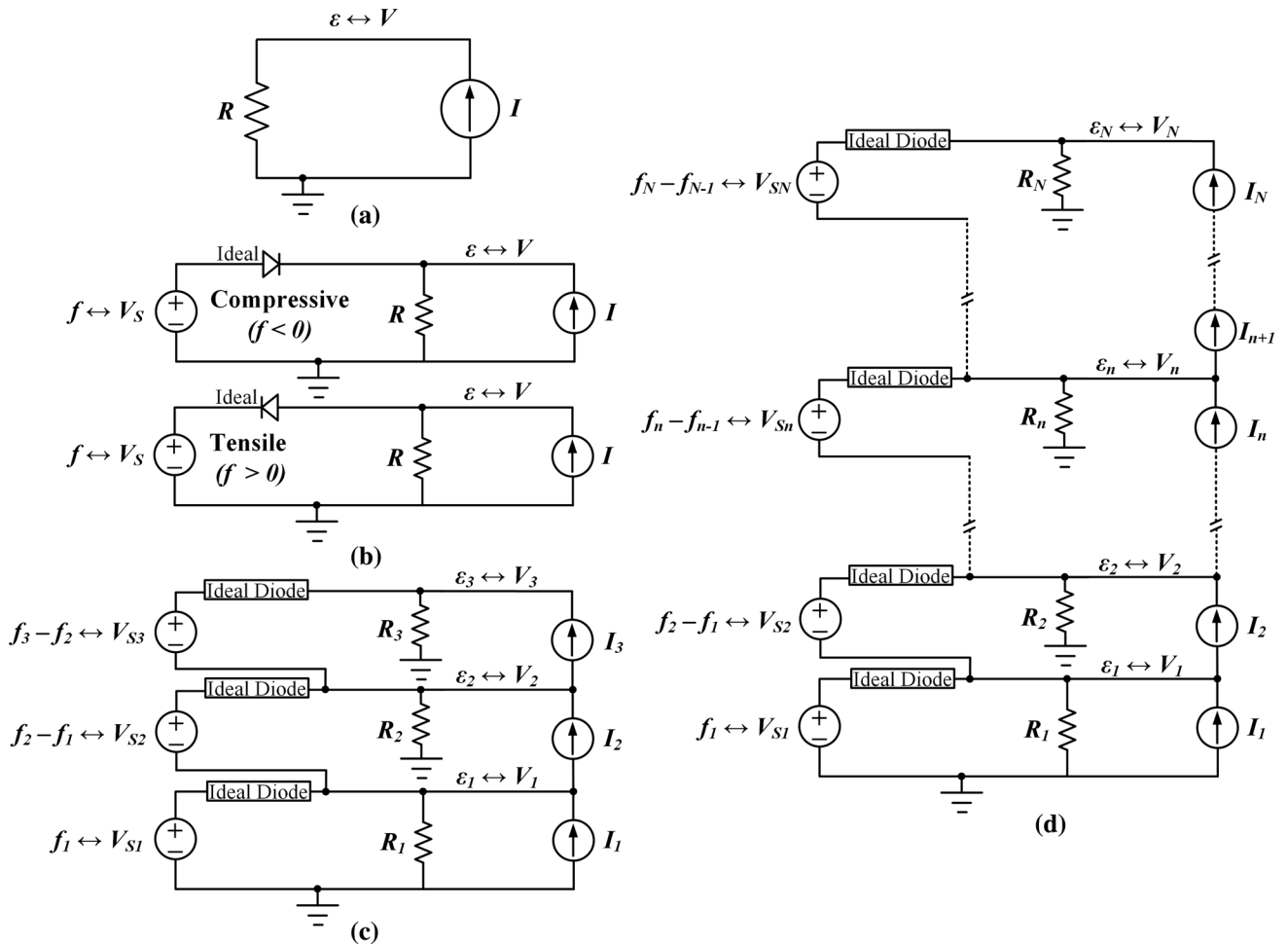


Fig. 2. (a) A simple resistive circuit comprising a resistor and an independent current source; (b) the equivalent electrical circuit to determine the equilibrium lattice relaxation of a single compositionally uniform epitaxial layer with either compressive and tensile cases; (c) the equivalent circuit for an epitaxial layer consisting of three sublayers with varying compositional mismatch and thickness; and (d) the equivalent circuit for an epitaxial layer broken down into N sublayers.

voltage expression for the top node of the simple electrical circuit shown in Fig. 2a:

$$\begin{aligned} 0 &= 2Yh\varepsilon - \frac{f}{|f|} \frac{Gb(1-\nu\cos^2\theta)}{2\pi(1-\nu)\sin\alpha\sin\phi} \left[\ln\left(\frac{h}{b}\right) + 1 \right] \\ &\leftrightarrow \frac{V}{R} - I = 0. \end{aligned} \quad (12)$$

The node voltage is determined from Kirchhoff's current law, which states that the algebraic sum of the currents flowing away from a node must equal zero.* In Eq. 12, the symbol \leftrightarrow implies that quantities or relationships on either side of the arrow are analogous though they generally possess different units. The derivative of the strain energy with respect to the in-plane strain is analogous to the current flowing through the resistor R , $\partial E_e/\partial\varepsilon \leftrightarrow I_R$, whereas the change in the dislocation energy with respect to the in-plane strain is analogous to the value of the independent current source I , $\partial E_D/\partial\varepsilon \leftrightarrow I$. Given that the partial derivatives are analogous to electrical currents, comparison of the two forms of Eq. 12 reveals that the equilibrium strain is analogous to the node voltage**:

$$\varepsilon \leftrightarrow V, \quad (13)$$

the factor multiplying the strain is analogous to a conductance (reciprocal of resistance):

$$2Yh \leftrightarrow \frac{1}{R}, \quad (14)$$

and the subtracted term is analogous to an independent current source entering the top node of the circuit (see Fig. 2a):

$$\frac{f}{|f|} \frac{Gb(1-\nu\cos^2\theta)}{2\pi(1-\nu)\sin\alpha\sin\phi} \left[\ln\left(\frac{h}{b}\right) + 1 \right] \leftrightarrow I. \quad (15)$$

To account for the possibility of pseudomorphic epitaxy, we can include an independent voltage source and an ideal diode[†] in the circuit, which together form a clipping circuit as shown in Fig. 2b. The ideal diode acts as a switch that is conductive

only when an epitaxial layer is coherently grown. The numerical value of the voltage source V_S is equal to the coherency strain in the layer:

$$f \leftrightarrow V_S. \quad (16)$$

To properly account for the sign of the lattice mismatch (tensile or compressive), the ideal diode must always face toward the *true positive terminal* of the independent voltage source (Fig. 2b illustrates both cases). Therefore, in terms of the electrical circuit model, the two analogous forms of the solution for the node voltage (or the equivalent equilibrium strain) are given as:

$$\begin{aligned} V &= \begin{cases} V_S, & h \leq h_c \\ I \cdot R, & h > h_c \end{cases} \leftrightarrow \varepsilon(h) \\ &= \begin{cases} f, & h \leq h_c \\ \frac{f}{|f|} \frac{b(1-\nu\cos^2\alpha)}{8\pi h(1+\nu)\sin\alpha\sin\phi} \left[\ln\left(\frac{h}{b}\right) + 1 \right], & h > h_c \end{cases}. \end{aligned} \quad (17)$$

During pseudomorphic epitaxy, the in-plane strain of the heterostructure is determined by the lattice mismatch, and, in the electrical circuit model, this is analogous to the conduction of an ideal diode connected in series with an independent voltage source. An ideal diode acts as a perfect conductor without any internal resistance which results in the formation of a supernode in the circuit shown on Fig. 2b; in other words, the separation of two essential nodes by an independent voltage source.

We can extend the electrical circuit model described above to the three-layer structure shown in Fig. 1b. By a similar approach, Eq. 10 resembles the node voltage expressions for three essential nodes[‡] and therefore we can consider the consecutive stacking of the electrical circuit given in Fig. 2b to obtain an equivalent circuit that describes a three-layered heterostructure (Fig. 2c). The appropriate connections of the electrical circuit block are done in such a way that the separation of two essential nodes consist on one end the combination of the independent voltage source and the ideal diode and in the other end the independent current source. Furthermore, in each building block, the resistor shares one of its terminals with the essential node and the other with the ground connection. Thus, in the analogous electrical circuit model, the node voltages for three essential nodes are given by

*In this analysis, an electrical current which enters the node is considered negative.

**It should be noted that the choice to represent the partial derivatives by analogous current sources is not unique, but was made for convenience. The analogous circuit could be defined differently and still yield the correct results, as long as a consistent set of analogs was used.

†An ideal diode acts as a switch which allows the flow of a forward bias current with any magnitude but which blocks current in the reverse bias direction.

‡An essential node is defined as a node connected to more than two circuit elements. Therefore, the number of essential nodes in the analogous circuit corresponds to the minimum number of equations which must be utilized to solve the circuit.

$$\begin{aligned}
 0 &= 2Y_3 h_3 \varepsilon_3 - \frac{f_3 - f_2}{|f_3 - f_2|} \frac{G_3 b_3 (1 - v_3 \cos^2 \alpha)}{2\pi(1 - v_3) \sin \alpha \sin \phi} \left[\ln \left(\frac{h_3}{b_3} \right) + 1 \right] && \leftrightarrow \frac{V_3}{R_3} - I_3 = 0 \\
 0 &= 2Y_2 h_2 \varepsilon_2 - \frac{f_2 - f_1}{|f_2 - f_1|} \frac{G_2 b_2 (1 - v_2 \cos^2 \alpha)}{2\pi(1 - v_2) \sin \alpha \sin \phi} \left[\ln \left(\frac{h_2 + h_3}{b_2} \right) + 1 \right] \\
 &+ \frac{f_3 - f_2}{|f_3 - f_2|} \frac{G_3 b_3 (1 - v_3 \cos^2 \alpha)}{2\pi(1 - v_3) \sin \alpha \sin \phi} \left[\ln \left(\frac{h_3}{b_3} \right) + 1 \right] && \leftrightarrow \frac{V_2}{R_2} - I_2 + I_3 = 0. \\
 0 &= 2Y_1 h_1 \varepsilon_1 - \frac{f_1 - f_0}{|f_1 - f_0|} \frac{G_1 b_1 (1 - v_1 \cos^2 \alpha)}{2\pi(1 - v_1) \sin \alpha \sin \phi} \left[\ln \left(\frac{h_1 + h_2 + h_3}{b_1} \right) + 1 \right] \\
 &+ \frac{f_2 - f_1}{|f_2 - f_1|} \frac{G_2 b_2 (1 - v_2 \cos^2 \alpha)}{2\pi(1 - v_2) \sin \alpha \sin \phi} \left[\ln \left(\frac{h_2 + h_3}{b_2} \right) + 1 \right] && \leftrightarrow \frac{V_1}{R_1} - I_1 + I_2 = 0
 \end{aligned} \tag{18}$$

It can be shown that the numerical value of the voltage at each node is equivalent to the equilibrium strain of that sublayer, $\varepsilon_1 \leftrightarrow V_1$, $\varepsilon_2 \leftrightarrow V_2$ and $\varepsilon_3 \leftrightarrow V_3$. In the three-layer system, the diode-connected independent voltage sources are determined by the difference in the lattice mismatch of the two adjacent layers where:

$$\begin{aligned}
 V_{S3} &\leftrightarrow f_3 - f_2 \\
 V_{S2} &\leftrightarrow f_2 - f_1. \\
 V_{S1} &\leftrightarrow f_1 - f_0
 \end{aligned} \tag{19}$$

For the case in which all sublayers are coherently grown, the diodes all operate in the forward conduction mode, and therefore the voltage at each essential node is determined by accounting for the sum of all the independent voltage sources up to and including the layer in consideration:

$$\begin{aligned}
 V_3 &= V_{S3} + V_{S2} + V_{S1} && \leftrightarrow \varepsilon_3 = f_3 \\
 V_2 &= V_{S2} + V_{S1} && \leftrightarrow \varepsilon_2 = f_2. \\
 V_1 &= V_{S1} && \leftrightarrow \varepsilon_1 = f_1
 \end{aligned} \tag{20}$$

Upon the growth of strained material in which misfit dislocation networks are present at each mismatched interface, the diodes are all in the reverse blocking mode (non-conductive), and the node voltages (layer strains) may be found by solution of the node voltage equations without inclusion of the independent voltage sources:

$$\begin{aligned}
 V_3 &= R_3 \cdot I_3 && \leftrightarrow \varepsilon_3 \\
 V_2 &= R_2 \cdot (I_2 - I_3) && \leftrightarrow \varepsilon_2. \\
 V_1 &= R_1 \cdot (I_1 - I_2) && \leftrightarrow \varepsilon_1
 \end{aligned} \tag{21}$$

In some cases, a coherent epitaxial layer may be grown on top of a metamorphic buffer. In such a case, the coherent interface, free from misfit dislocations, corresponds to a conducting diode in the electrical circuit. The presence of one or more interfaces free from misfit dislocations can be described by the existence of a misfit dislocation free zone. The conduction of the diode results in the connection of an independent voltage source directly between essential nodes, which in circuit theory can be considered to form a supernode.[§] In other words, the presence of a MDFZ may be likened to the formation of a supernode in electrical circuit theory.

[§]A supernode in electrical circuit theory refers to the case where two essential nodes are separated by an independent voltage source.

The existence of the supernode modifies the node voltage equations for the nodes involved, and therefore the resulting node voltages, which will be described in more detail below when considering the general treatment of an arbitrary heterostructure.

In the most general case, where we can consider an arbitrary heterostructure consisting of multiple and/or compositionally-graded epitaxial layers as shown in Fig. 1c, we can extend the above analysis by dividing the epitaxial layer into N disparate sublayers (Fig. 2d). The partial derivatives shown in Eq. 11 are given in terms of their analogous electrical circuit components as

$$\begin{aligned}
 0 &= 2Y_n h_n \varepsilon_n - \frac{f_n - f_{n-1}}{|f_n - f_{n-1}|} \frac{G_n b_n (1 - v_n \cos^2 \alpha)}{2\pi(1 - v_n) \sin \alpha \sin \phi} \left[\ln \left(\frac{h_n}{b_n} \right) + 1 \right] && \leftrightarrow \frac{V_n}{R_n} - I_n = 0, \quad n = N \\
 0 &= \left(2Y_n h_n \varepsilon_n - \frac{f_n - f_{n-1}}{|f_n - f_{n-1}|} \frac{G_n b_n (1 - v_n \cos^2 \alpha)}{2\pi(1 - v_n) \sin \alpha \sin \phi} \left[\ln \left(\sum_{j=n}^N \frac{h_j}{b_n} \right) + 1 \right] \right) \\
 &+ \left(\frac{f_{n+1} - f_n}{|f_{n+1} - f_n|} \frac{G_{n+1} b_{n+1} (1 - v_{n+1} \cos^2 \alpha)}{2\pi(1 - v_{n+1}) \sin \alpha \sin \phi} \left[\ln \left(\sum_{j=n+1}^N \frac{h_j}{b_{n+1}} \right) + 1 \right] \right) && \leftrightarrow \frac{V_n}{R_n} - I_n + I_{n+1} = 0, \quad 1 \leq n < N
 \end{aligned} \tag{22}$$

In this extended analogy, the n th sublayer may be modeled by an electrical subcircuit in which:

$$R_n \leftrightarrow \frac{1}{2Y_n h_n}, \quad 1 \leq n \leq N, \tag{23}$$

$$I_n \leftrightarrow \frac{f_n - f_{n-1}}{|f_n - f_{n-1}|} \frac{G_n b_n (1 - v_n \cos^2 \theta)}{2\pi(1 - v_n) \sin \alpha \sin \phi} \left[\ln \left(\sum_{j=n}^N \frac{h_j}{b_n} \right) + 1 \right], \quad 1 \leq n \leq N, \tag{24}$$

and

$$V_{Sn} \leftrightarrow f_n - f_{n-1}, \quad 1 \leq n \leq N, \tag{25}$$

The ideal diode in each sublayer is always facing the *true positive terminal* of the independent voltage source at that sublayer; when the diode conducts, the independent voltage source is dissipative. In the case in which each sublayer contains misfit dislocations, none of the diodes conduct, and the in-plane strain (node voltage) at the n th sublayer is determined by

$$\varepsilon_n \leftrightarrow V_n = \begin{cases} R_n \cdot (I_n - I_{n+1}), & 1 \leq n < N \\ R_n \cdot I_n, & n = N \end{cases}. \tag{26}$$

The linear misfit dislocation density at each sublayer may then be determined by

Table I. Material properties for InAs, GaAs and the alloy $\text{In}_x\text{Ga}_{1-x}\text{As}$ ²⁵ where a is the lattice constant, C_{11} and C_{12} are the elastic stiffness constants and x is the indium mole fraction

Material	Parameter		
	a (nm)	C_{11} (GPa)	C_{12} (GPa)
InAs	0.60584	83.3	45.3
GaAs	0.56534	118.4	53.7
$\text{In}_x\text{Ga}_{1-x}\text{As}$	$0.56534 + x(0.0405)$	$118.4 - x(35.1)$	$53.7 - x(8.4)$

Linear interpolation following Vegard's law was used to determine the material properties of the $\text{In}_x\text{Ga}_{1-x}\text{As}$ alloy.

RESULTS AND DISCUSSION

In applying the electrical circuit model to multi-layered heterostructures and comparing its results to the numerical minimum energy calculations, we considered the following cases (Table I).

Uniform Composition Layers

The simplest structure is one composed of three pseudomorphic layers in which the whole structure is coherently grown on the substrate. Figure 3a shows a multilayered $\text{In}_x\text{Ga}_{1-x}\text{As}/\text{GaAs}$ (001) heterostructure (Sample A) consisting of three uniform and pseudomorphic layers with indium compositions of $x_1 = 1\%$, $x_2 = 3\%$ and $x_3 = 5\%$, respectively, and thicknesses of $h_1 = 10$ nm, $h_2 = 5$ nm and $h_3 = 10$ nm, respectively. Figure 3b illustrates the equivalent electrical circuit model for the entire structure; the numerical values for the electrical components used here are summarized in Table II. Given that the thickness of each layer is below the critical thickness for misfit dislocation formation, the in-plane strain at each sublayer is equal to the coherency strain and therefore its lattice mismatch. In the equivalent electrical circuit model, the ideal diode at each node is conductive and therefore the respective current sources play no role in determining the voltage (i.e., in-plane strain) at each node. Furthermore, the voltage at each node is determined from the sum of all voltage sources up to and including the layer under consideration. The numerical value of the voltage in node one is equal to the lattice mismatch of sublayer one, the voltage at node two is equal to the sum of the voltage sources for sublayers one and two, and the voltage at node three is equal to the sum of all three voltage sources. Therefore, the numerical value of the voltage at each node is equal to the lattice mismatch of that layer as expressed by $\varepsilon_n = f_n \leftrightarrow V_n = V_{\text{Sn}}$. As shown in Table III, the results obtained for Sample A using the circuit model agree with results from the numerical energy minimization approach.

The growth of mismatched epilayers which are beyond the critical layer thickness requires the formation of a misfit dislocation network to relax

$$\rho_n = \frac{f_n - f_{n-1}}{|f_n - f_{n-1}|} \frac{(f_n - \varepsilon_n) - (f_{n-1} - \varepsilon_{n-1})}{b_n \sin \alpha \sin \phi}, \quad 1 \leq n \leq N. \quad (27)$$

From a fabrication point of view, the growth of mismatched and compositionally-graded epitaxial layers yields metamorphic heterostructures which may contain misfit dislocation free zones. In this situation, where the epitaxial structure as a whole is incoherent but some of the sublayers are coherently grown with respect to the ones below, the presence of a misfit dislocation free zone is equivalent to the formation of a supernode in the analogous electrical circuit model. Therefore, the node voltage (or the equivalent in-plane strain) in the bottom layer of the supernode is determined by accounting for the equivalent resistance of all the layers included in the supernode. If the supernode is bounded inclusively by sublayers σ and ω , then the equilibrium strain (node voltage) in the bottom layer of the supernode is given by

$$\varepsilon_\sigma \leftrightarrow V_\sigma = \left[(I_\sigma - I_{\omega+1}) - \sum_{j=\sigma}^{\omega} \frac{\sum_{i=1}^j V_{Si} - \sum_{i=1}^{\sigma} V_{Si}}{R_j} \right] R_{\text{SN}}, \quad (28)$$

where the equivalent parallel resistance of the supernode (R_{SN}) is defined as the equivalent resistance for a series of resistors in parallel, $R_{\text{SN}} = R_\sigma || \dots || R_\omega$, and is given by

$$R_{\text{SN}} = \left(\sum_{j=\sigma}^{\omega} \frac{1}{R_j} \right)^{-1}. \quad (29)$$

The in-plane strain (node voltage) at each sublayer of the *supernode* is then determined by adding the appropriate sum of independent voltage sources to the voltage at the bottom of the supernode. In other words, the node voltage (or the equivalent in-plane strain) of each sublayer of the *supernode* is determined from

$$\varepsilon_i = \varepsilon_\sigma + \sum_{j=\sigma+1}^i f_j - f_{j-1} \leftrightarrow V_i = V_\sigma + \sum_{j=\sigma+1}^i V_{Sj}, \quad \sigma < i \leq \omega, \quad (30)$$

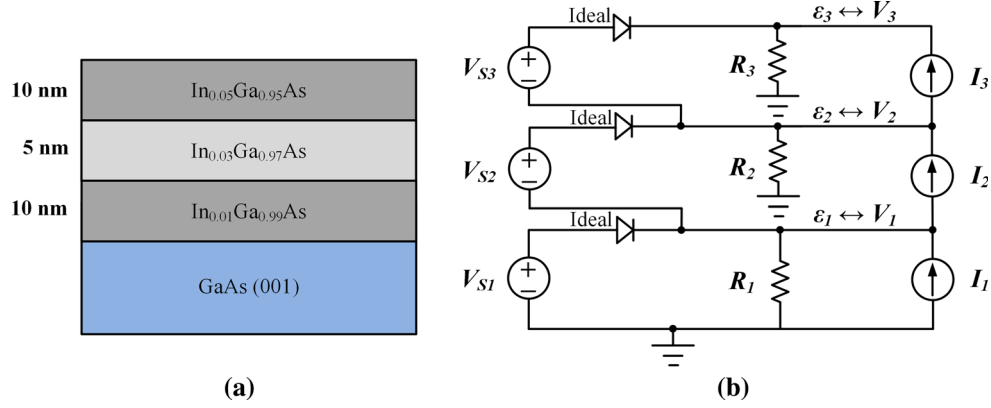


Fig. 3. (a) Schematic representation of a coherently-grown multilayer heterostructure with three compositionally uniform epitaxial layers consisting of 10 nm $\text{In}_{0.05}\text{Ga}_{0.95}\text{As}$ /5 nm $\text{In}_{0.03}\text{Ga}_{0.97}\text{As}$ /10 nm $\text{In}_{0.01}\text{Ga}_{0.99}\text{As}$ on a GaAs (001) substrate. (b) The equivalent electrical circuit for the multilayer heterostructure consisting of the series connection (stacking) of the electrical circuit blocks where the material properties of each sublayer are modeled using the equivalent electrical components (resistor, ideal diode, independent current and independent voltage sources).

Table II. The numerical values of the electrical components for the electrical circuits

Sample	Resistance ($\text{n}\Omega$)	Voltage source (mV)	Current source (kA)
A (Fig. 3b)	$R_1 = 406.6$	$V_{S1} = -0.716$	$I_1 = -28.217$
	$R_2 = 818.9$	$V_{S2} = -1.428$	$I_1 = -25.246$
	$R_3 = 412.4$	$V_{S3} = -1.425$	$I_1 = -22.881$
B (Fig. 4b)	$R_1 = 55.97$	$V_{S1} = -7.1$	$I_1 = -41.098$
	$R_2 = 45.25$	$V_{S2} = -13.9$	$I_1 = -37.022$
	$R_3 = 28.50$	$V_{S3} = 10.4$	$I_1 = 36.352$
C (Fig. 5b)	$R_1 = 83.96$	$V_{S1} = -7.1$	$I_1 = -41.494$
	$R_2 = 83.96$	$V_{S2} = 0$	$I_1 = 0$
	$R_3 = 83.96$	$V_{S3} = 0$	$I_1 = 0$
D (Fig. 6b)	$R_1 = 406.6$	$V_{S1} = -0.716$	$I_1 = -38.385$
	$R_2 = 408.0$	$V_{S2} = -0.715$	$I_2 = -35.144$
	$R_3 = 409.5$	$V_{S3} = -0.714$	$I_3 = -34.388$
	$R_4 = 410.9$	$V_{S4} = -0.713$	$I_4 = -33.550$
	$R_5 = 412.4$	$V_{S5} = -0.712$	$I_5 = -32.605$
	$R_6 = 413.8$	$V_{S6} = -0.711$	$I_6 = -31.513$
	$R_7 = 415.3$	$V_{S7} = -0.710$	$I_7 = -30.206$
	$R_8 = 416.8$	$V_{S8} = -0.709$	$I_8 = -28.560$
	$R_9 = 418.3$	$V_{S9} = -0.708$	$I_9 = -26.292$
	$R_{10} = 419.8$	$V_{S10} = -0.707$	$I_{10} = -22.502$

Table III. The in-plane strains of various multilayered heterostructures and comparisons between numerical minimum energy results and the electrical circuit model

Sample	Numerical minimum energy	Electrical circuit model
A (Fig. 3a)	$\epsilon_3 = -0.3569\%$	$\epsilon_3 = -0.3569\%$
	$\epsilon_2 = -0.2144\%$	$\epsilon_2 = -0.2144\%$
B (Fig. 4a)	$\epsilon_1 = -0.0716\%$	$\epsilon_1 = -0.0716\%$
	$\epsilon_3 = +0.1035\%$	$\epsilon_3 = +0.1035\%$
C (Fig. 5a)	$\epsilon_2 = -0.3267\%$	$\epsilon_2 = -0.3267\%$
	$\epsilon_1 = -0.0228\%$	$\epsilon_1 = -0.0228\%$
	$\epsilon_3 = -0.0499\%$	$\epsilon_3 = -0.0498\%$
	$\epsilon_2 = -0.0499\%$	$\epsilon_2 = -0.0498\%$
	$\epsilon_1 = -0.0499\%$	$\epsilon_1 = -0.0498\%$

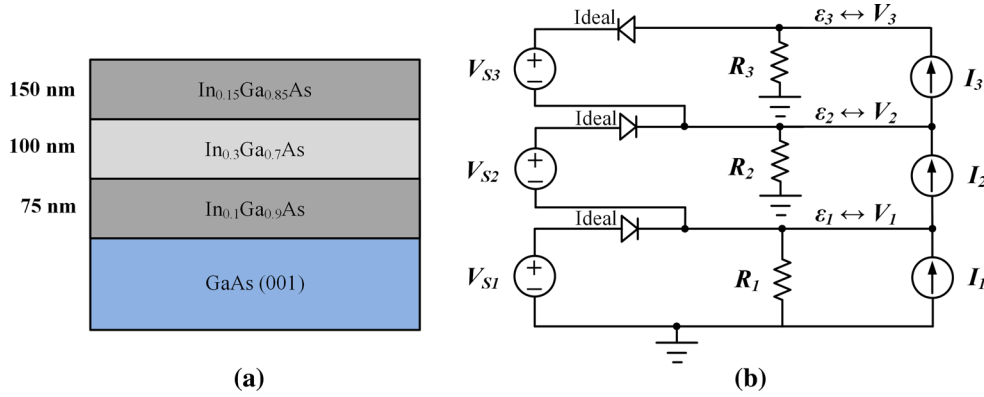


Fig. 4. (a) Schematic representation of an incoherently-grown multilayer heterostructure with three compositionally uniform epitaxial layers consisting of 150 nm $\text{In}_{0.15}\text{Ga}_{0.85}\text{As}$ /100 nm $\text{In}_{0.3}\text{Ga}_{0.7}\text{As}$ /75 nm $\text{In}_{0.1}\text{Ga}_{0.9}\text{As}$ on a GaAs (001) substrate. (b) The equivalent electrical circuit for the multilayer heterostructure consisting of the series connection (stacking) of the electrical circuit blocks where the material properties of each sublayer are modeled using the equivalent electrical components (resistor, ideal diode, independent current and independent voltage sources).

some portion of the lattice mismatch. In uniform layers, misfit dislocations are introduced at the mismatched interfaces and they can be modeled using the Dirac delta function. The heterostructure shown in Fig. 4a includes three incoherently-grown and mismatched sublayers with lattice mismatch $f_1 = -0.71\%$, $f_2 = -2.1\%$ and $f_3 = -1.06\%$ and thicknesses $h_1 = 75$ nm, $h_2 = 100$ nm and $h_3 = 150$ nm. The analogous electrical circuit is shown in Fig. 4b. The numerical minimum energy results shown in Table III for Sample B suggest that all three sublayers are partly relaxed and all interfaces contain misfit dislocation networks. It is interesting to note that sublayers one and two exhibit compressive strain, similar to the lattice mismatch, whereas sublayer three exhibits tensile strain which is opposite to the lattice mismatch; the tensile strain present in the third sublayer suggests that misfit dislocations with Burgers vectors opposite in sense to those at the other two interfaces have been introduced. Standard electrical circuit simulator (SECS) modeling results of the electrical circuit shown in Fig. 4b are in excellent agreement with minimum energy calculations. Furthermore, diodes at each node are non-conductive and therefore the node voltage is determined by the sum of the currents flowing through that node and the resistor attached to it. Thus, the voltage (in-plane strain) at each node is given by

$$\begin{aligned} \varepsilon_3 &= +0.1035\% \leftrightarrow V_3 = R_3 \cdot I_3 = +1.035 \text{ mV} \\ \varepsilon_2 &= -0.3267\% \leftrightarrow V_2 = R_2 \cdot (I_2 - I_3) = -3.267 \text{ mV} \\ \varepsilon_1 &= -0.0228\% \leftrightarrow V_1 = R_1 \cdot (I_1 - I_2) = -0.228 \text{ mV} \end{aligned} \quad (31)$$

For the third heterostructure, we considered the important case of a single uniform and incoherently-grown epitaxial layer as shown in Fig. 5a with a total thickness of $h = 350$ nm and a lattice mismatch of $f = -0.71\%$. For the purpose of illustration, and also to provide a stringent test of the

electrical circuit model, we divided the epitaxial layer into three sublayers with varying thicknesses ($h_1 = 50$ nm, $h_2 = 200$ nm and $h_3 = 100$ nm), but each sublayer contained the same composition (and therefore the same lattice mismatch with respect to the substrate). The in-plane strain of the heterostructure considered in Fig. 5a could be easily calculated using the well-known Matthews and Blakeslee's model (Eq. 4) by considering the total epitaxial thickness. The equilibrium in-plane strain determined for Sample C (Table III) from all three models are in excellent agreement. In addition, SECS modeling of the electrical circuit shown in Fig. 5c indicates that the ideal diode at sublayer one is non-conductive, which suggests the presence of a misfit dislocation network at the substrate interface. However, at the second and third nodes, the ideal diodes are conductive; diode conduction at nodes two and three indicates the presence of a misfit dislocation free zone in the epitaxial sublayers two and three and implies that a three-fold supernode will be formed. As a consequence of the supernode formation, the current source at node one (I_1) flows through resistors R_1 , R_2 and R_3 arranged in parallel (Fig. 5c); the voltage at each node is determined from the product of the current source I_1 and the equivalent parallel resistance $R_1 || R_2 || R_3$. Thus, the in-plane strain of each sublayer is given as:

$$\begin{aligned} \varepsilon_1 = \varepsilon_2 = \varepsilon_3 &= -0.0498\% \leftrightarrow V_1 = V_2 \\ &= V_3 = \left(\frac{1}{R_1} + \frac{1}{R_2} + \frac{1}{R_3} \right)^{-1} I_1 = -0.498 \text{ mV}. \end{aligned} \quad (32)$$

Step-Graded Epitaxial Layers

The electrical circuit model could be extended to any arbitrary multilayered heterostructure employing compositional-grading. Figure 6a illustrates a step-graded buffer comprising ten uniform layers

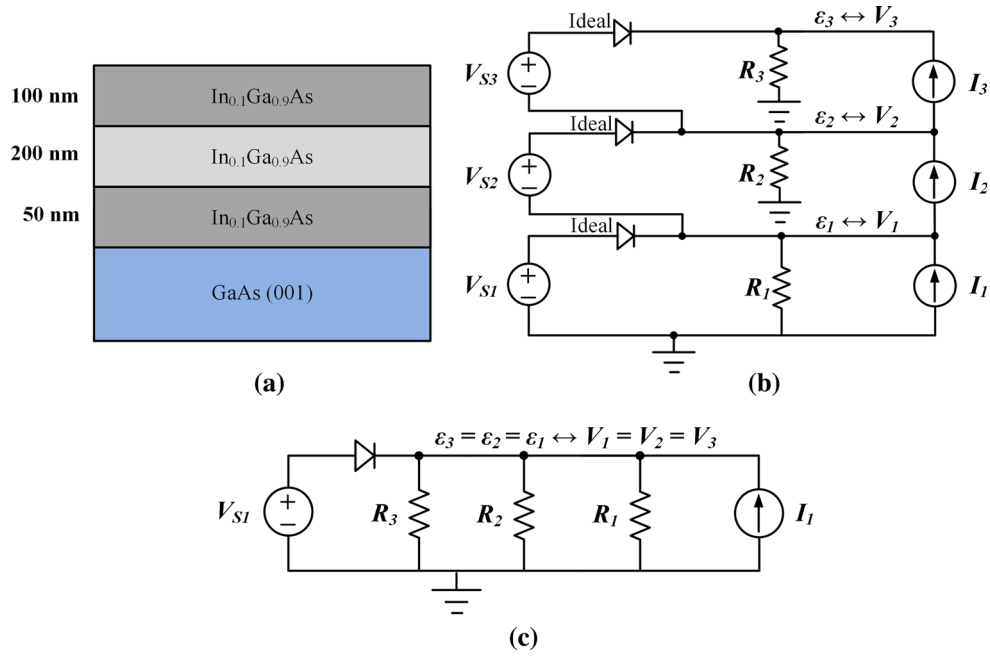


Fig. 5. (a) Schematic representation of an incoherently-grown multilayer heterostructure with three sublayers where the top two are coherently-grown. Physically, the heterostructure can be considered as a single compositionally uniform 350-nm-thick $\text{In}_{0.1}\text{Ga}_{0.9}\text{As}$ layer deposited on a GaAs (001) substrate; however, for the purpose of illustration, it is broken down to 100-nm $\text{In}_{0.1}\text{Ga}_{0.9}\text{As}$ /200-nm $\text{In}_{0.1}\text{Ga}_{0.9}\text{As}$ /50-nm $\text{In}_{0.1}\text{Ga}_{0.9}\text{As}$. (b) The equivalent electrical circuit for the multilayer heterostructure consisting of the series connection (stacking) of three electrical circuit blocks where the material properties of each sublayer are modeled using the equivalent electrical components (resistor, ideal diode, independent current and independent voltage sources).

each with 10 nm thickness, and in which there are equal compositional changes from one layer to the next (linear step-grading). For the structure studied here, the indium composition is varied from 1% at the sublayer closest to the substrate interface to a final surface indium composition of 10% corresponding to a lattice mismatch of 0.71%; the lattice mismatch profile as a function of the distance from the substrate interface z is shown in Fig. 6c (dashed line). The corresponding electrical circuit is illustrated in Fig. 6b. For the case of a step-graded layer consisting of N sublayers, the maximum number of mismatched interfaces is equal to the number of mismatched interfaces (10 in the current case). Kujofsa and Ayers^{8,9} have shown that, in general, continuously-graded layers contain misfit dislocation free zones adjacent to the substrate interface and surface, provided that there is zero interfacial mismatch and/or the grading coefficient is sufficiently small. However, in step-graded layers, the thicknesses of the interfacial and surface misfit dislocation free zones are constrained to be related to multiples of the step-layer thickness, which in this case is one tenth of the total buffer layer thickness ($h_T = 100$ nm).¹⁰ In $\text{In}_x\text{Ga}_{1-x}\text{As}/\text{GaAs}$ (001) step-graded layers, the presence of an interfacial MDFZ is evident only when a very small grading coefficient is used (approximately 2% indium per micron). In addition, for a low ending composition, and therefore ending lattice mismatch,

the surface misfit dislocation free zone may extend beyond the top step layer.

Figure 6c depicts the equilibrium in-plane strain distribution determined by numerical minimum energy calculations (solid lines) and the electrical circuit (circle symbols) as a function of the distance from the interface. The in-plane strain profile comprises a series of step functions with discontinuities at the mismatched interfaces. The first five interfaces contain misfit dislocations which relax most of the mismatch strain and result in small values of the residual strain. The absence of misfit dislocation networks at the top five interfaces results in high built-in strains. These results from the circuit analysis are in excellent agreement with numerical energy minimization calculations, as shown in Fig. 6c.

Linearly-Graded Epitaxial Layers

The electrical circuit model could be applied to any heterostructure with an arbitrary number of sublayers. Figure 7 illustrates the lattice mismatch profile and equilibrium strain for a linearly-graded layer of $\text{In}_x\text{Ga}_{1-x}\text{As}$ grown epitaxially on a GaAs (001) substrate. Here, the dashed line shows the profile of lattice mismatch, which varies linearly from zero (corresponding to zero indium mole fraction) to $f_h = -0.71\%$ at the surface (corresponding to 10% indium mole fraction). Figure 7 also shows the equilibrium strain profile for the linearly-

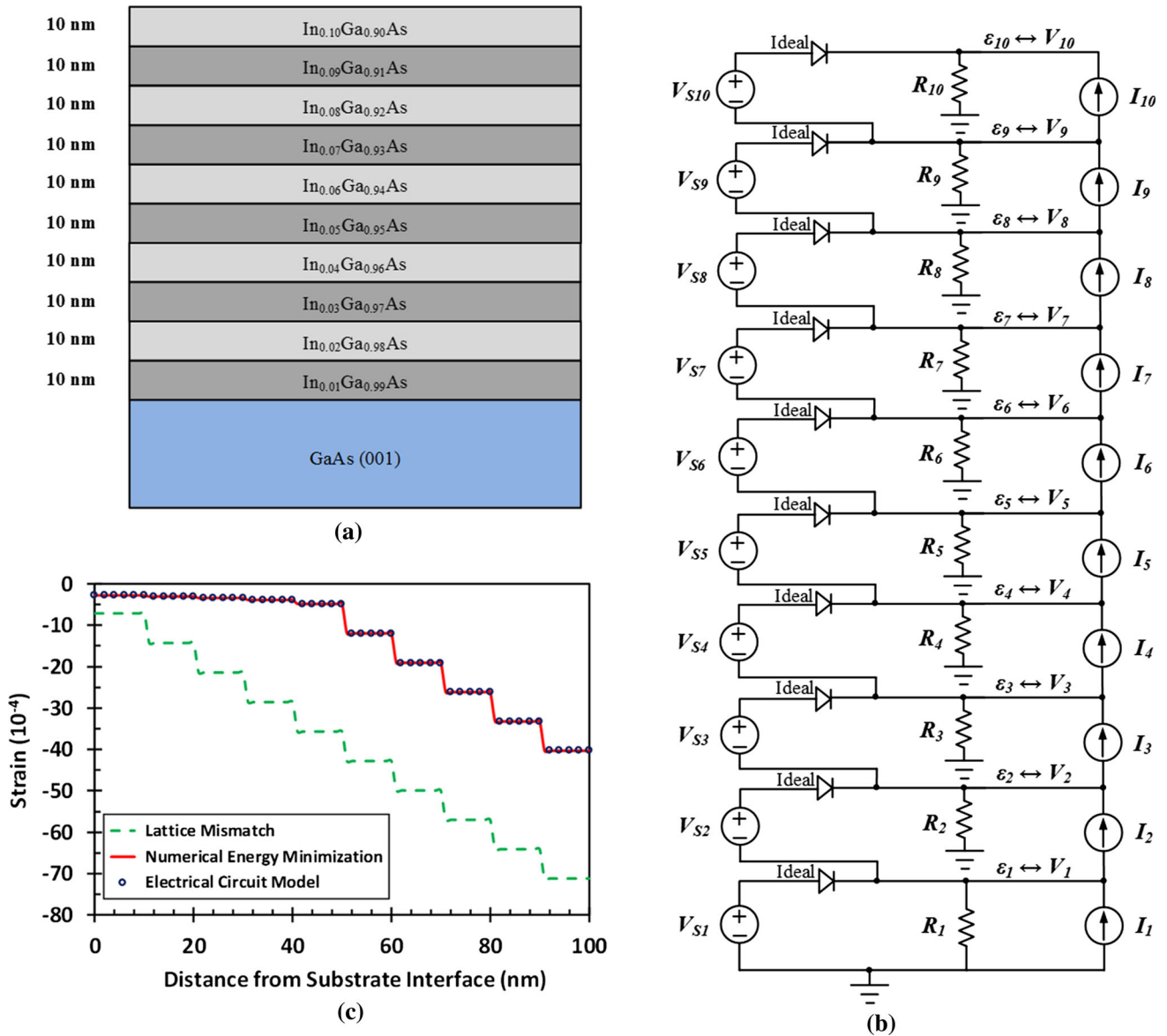


Fig. 6. (a) Schematic representation of 100-nm-thick step-graded $\text{In}_{0.1}\text{Ga}_{0.9}\text{As}$ epitaxial layer with 10 sublayers where the indium composition is varied in steps of 1% starting from 1% at the sublayer nearest the interface and ending at 10% in the sublayer at the surface. (b) The equivalent electrical circuit for the step-graded heterostructure consisting of the series connection (stacking) of 10 electrical circuit blocks where the material properties of each sublayer are modeled using the equivalent electrical components (resistor, ideal diode, independent current and independent voltage sources). (c) Lattice mismatch (dashed) and in-plane strain (solid, circle) as a function of the distance from the interface for the step-graded epilayer. The in-plane strain is determined using the numerical minimum energy (solid line) and electrical circuit (open circles) models.

graded layer, as determined by numerical minimum energy calculations (solid line) and the electric circuit model (open circles). These two results are in excellent agreement, and both show the existence of an interfacial misfit dislocation free zone as well as a surface misfit dislocation free zone, as expected on the basis of previous studies.^{7,9–11} The misfit dislocation free zones exhibit residual strain profiles with the same slope as the lattice mismatch, and exhibit widths of 5 nm (at the interface) and 46 nm (at the surface). Between these, there is a dislocated region of thickness 49 nm in which the strain is nearly constant.

In our work, the fundamental equations for the strain energy and dislocation line energy are essentially the same as those used by Matthews,¹⁵ and later by Tersoff^{13,14}. Although the equilibrium configuration in the linearly-graded epitaxial layer has been explored in great detail by Tersoff,^{13,14} Fitzgerald et al.²⁶ Dunstan²⁷ and Romano et al.,²⁸ these models assume that graded material can relax completely in the presence of misfit dislocations. This is a simplifying assumption which does not strictly hold in either equilibrium or kinetically-limited relaxation. More specifically, there are two key assumptions embedded in these models: first,

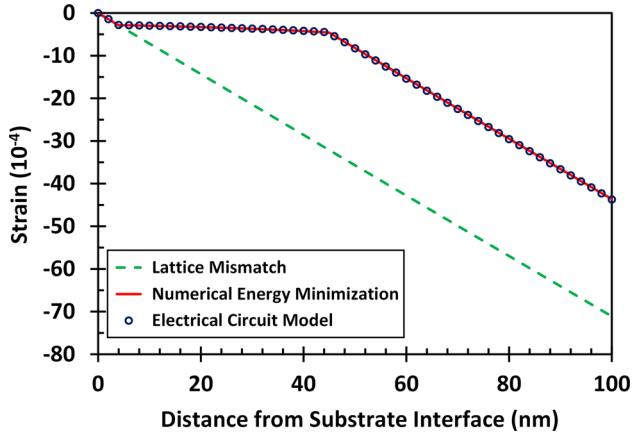


Fig. 7. Lattice mismatch (dashed) and in-plane strain (solid, circles) as a function of the distance from the interface for a 100-nm-thick linearly-graded $\text{In}_x\text{Ga}_{1-x}\text{As}$ epitaxial layer where the indium composition is varied linearly from 0 at the substrate interface to 10% at the surface. The in-plane strain is determined using the numerical minimum energy (solid line) and electrical circuit (open circles) models.

there is zero strain in the dislocated region; and second, they neglect the thickness dependence of the line energies for dislocations. As a consequence of these simplifying assumptions, the interfacial misfit dislocation-free zone is not seen and there is zero strain in the dislocated region. Therefore, the in-plane strain characteristic is described by these models as,

$$\varepsilon(z) = \begin{cases} 0 & z \leq z_c; \\ C_f(z - z_c) & z_c < z \leq h. \end{cases} \quad (33)$$

where z_c is the edge of the dislocated region near the surface and C_f is the grading coefficient. The numerical and the equivalent electrical circuit models do not make such simplifying assumptions, and therefore the residual strain characteristics is slightly different from the previously developed models. If the edges of the interfacial and surface MDFZs are located at distances of z_1 and z_2 from the substrate interface, as illustrated in Fig. 7, and therefore the misfit dislocation density is concentrated in the middle region ($z_1 \leq z \leq z_2$), then the residual strain can be analytically modeled as follows: in the interfacial MDFZ, the absence of misfit dislocations indicates that the residual strain is equal to the lattice mismatch profile and therefore:

$$\varepsilon(z) = C_f z, \quad z \leq z_1. \quad (34)$$

In the dislocated region ($z_1 \leq z \leq z_2$), the residual strain is modeled by the electrical circuit model as

$$\varepsilon_n \leftrightarrow V_n = R_n \cdot (I_n - I_{n+1}). \quad (35)$$

An important application of the electric circuit model analogy is to the case of a continuously-graded layer. This can be considered by approximating the continuously-graded material by a stack of uniform

composition sublayers and then taking the limit as the thickness of the individual sublayers approaches zero. This development is similar to the transition from electric circuit theory using lumped circuit elements to electromagnetic theory using distributed electrical quantities. This enables the development of analytical expressions for the strain, misfit dislocation density, critical layer thickness and widths of misfit dislocation free zones in a continuously-graded layer having any arbitrary compositional profile. Previously, only the linear²² and exponential²³ grading cases had been considered theoretically, but the circuit model analogy allows the analysis of any continuously-graded layer, including those with power law, S-graded, or some type of non-linear compositional profiles. This development will be described below.

Using the electric circuit analogy and assuming that the physical constants b , ν , G and Y are slowly varying functions of n , the in-plane strain in the n^{th} sublayer is given by

$$\varepsilon_n = -\frac{1}{2Y_n h_n} \left\{ \begin{aligned} & \frac{f_n - f_{n-1}}{|f_n - f_{n-1}|} \frac{Gb(1 - \nu \cos^2 \alpha)}{2\pi(1 - \nu) \sin \alpha \sin \phi} \left[\ln \left(\sum_{j=n}^N \frac{h_j}{b} \right) + 1 \right] \\ & - \frac{f_{n+1} - f_n}{|f_{n+1} - f_n|} \frac{Gb(1 - \nu \cos^2 \alpha)}{2\pi(1 - \nu) \sin \alpha \sin \phi} \left[\ln \left(\sum_{j=n+1}^N \frac{h_j}{b} \right) + 1 \right] \end{aligned} \right\}. \quad (36)$$

As a specific example for a monotonic continuously-graded layer $\frac{f_n - f_{n-1}}{|f_n - f_{n-1}|} = \frac{f_{n+1} - f_n}{|f_{n+1} - f_n|}$. Thus

$$\varepsilon_n = \frac{1}{2Y h_n} \frac{f_{n+1} - f_n}{|f_{n+1} - f_n|} \frac{Gb(1 - \nu \cos^2 \alpha)}{2\pi(1 - \nu) \sin \alpha \sin \phi} \ln \left(\frac{\sum_{j=n}^N \frac{h_j}{b}}{\sum_{j=n+1}^N \frac{h_j}{b}} \right). \quad (37)$$

Equation 37 can be simplified to

$$\varepsilon_n = \frac{1}{2Y} \frac{f_{n+1} - f_n}{|f_{n+1} - f_n|} \frac{Gb(1 - \nu \cos^2 \alpha)}{2\pi(1 - \nu) \sin \alpha \sin \phi} \frac{\ln \left(\frac{h_n + h - z}{h_n} \right)}{h_n}, \quad (38)$$

where h is the epitaxial layer thickness and z is the distance from the substrate interface to the top of layer n . For simplicity let

$$A = \frac{1}{2Y} \frac{f_{n+1} - f_n}{|f_{n+1} - f_n|} \frac{Gb(1 - \nu \cos^2 \alpha)}{2\pi(1 - \nu) \sin \alpha \sin \phi}. \quad (39)$$

The limiting case of a continuously-graded layer, in which $h_n \rightarrow 0$, may be understood using L'Hopital's rule, giving

$$\begin{aligned} \lim_{h_n \rightarrow 0} \{\varepsilon_n\} &= \lim_{h_n \rightarrow 0} \left\{ \frac{A \frac{\partial}{\partial h_n} \left[\ln \left(\frac{h_n + h - z}{h_n} \right) \right]}{\frac{\partial}{\partial h_n} [h_n]} \right\} \\ &= \lim_{h_n \rightarrow 0} \left\{ \frac{A}{h_n + h - z} \right\} = \frac{A}{h - z} = \varepsilon(z). \end{aligned} \quad (40)$$

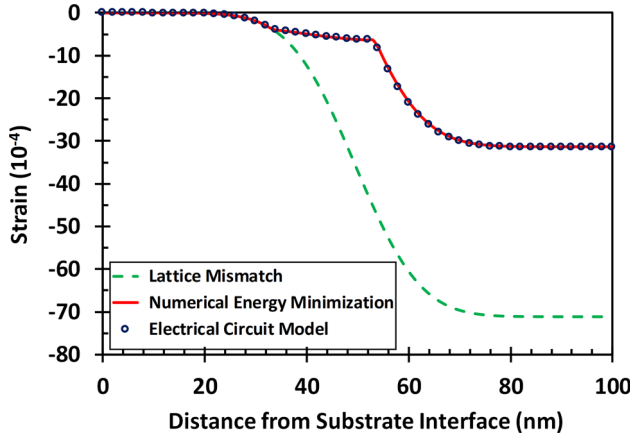


Fig. 8. Lattice mismatch (dashed) and in-plane strain (solid, circles) as a function of the distance from the interface for a 100-nm-thick S-graded epilayer $\text{In}_x\text{Ga}_{1-x}\text{As}$ epitaxial layer where the indium composition is varied linearly from 0 at the substrate interface to 10% at the surface. The mean parameter was fixed at half of the epitaxial layer thickness $\mu = 50$ nm, and the standard deviation parameter was $\sigma = 10$ nm. The in-plane strain is determined using the numerical minimum energy (solid line) and electrical circuit (open circles) models.

Therefore, in the dislocated region of any continuously-graded layer, the in-plane strain will have this dependence on distance from the interface, apart from small compositional variations in b , v , G and Y . This contrasts with simple models previously developed in which it was assumed that the dislocated region of a graded layer would be unstrained. The characteristic of Eq. 40 describes the residual strain in structures where the misfit dislocation region extends all the way to the substrate interface, however, in linearly-graded epitaxial layers, the presence of the interfacial MDFZ leads to the adjustment of the strain profile. In addition, the strain characteristics described here accounts for the variation of the residual strain in the dislocated region. Thus, the in-plane strain in the dislocated region is modeled by

$$\varepsilon(z) = \frac{A}{h-z} - \frac{A}{h} + C_f z_1, \quad z_1 < z \leq z_2. \quad (41)$$

The second and third terms in the equation above represent adjustments to account for the strain at the top of the interfacial MDFZ. By a similar analysis, in the surface MDFZ, the absence of misfit dislocations implies that the residual strain is proportional to the lattice mismatch and therefore the strain in this region is given by

$$\varepsilon(z) = C_f(z - z_2) + \frac{A}{h-z_2} - \frac{A}{h} + C_f z_1, \quad z_2 < z \leq h. \quad (42)$$

Therefore, according to this model, the equilibrium strain profile in the linearly-graded layer is given by

$$\varepsilon(z) = \begin{cases} C_f z & z \leq z_1; \\ A \frac{z}{h(h-z)} + C_f z_1 & z_1 < z \leq z_2; \text{ and} \\ C_f(z - z_2) + A \frac{z_2}{h(h-z_2)} + C_f z_1 & z_2 < z \leq h. \end{cases} \quad (43)$$

The equation for the surface MDFZ boundary z_2 is given by

$$\int_{z_2}^h \varepsilon(z) dz = \frac{E_d}{2b'Y} = \int_{z_2}^h C_f(z - z_2) + \varepsilon(z_2) dz \quad (44)$$

$$= A \left[\ln\left(\frac{h-z_2}{b}\right) + 1 \right].$$

Solving the expression above and recognizing that the width of the surface MDFZ is $W_{\text{MDFZ}} = h - z_2$, yields

$$W_{\text{MDFZ}} = \sqrt{\frac{2A}{C_f} \left[\ln\left(\frac{W_{\text{MDFZ}}}{b}\right) + 1 \right] + 2 \frac{Az_2}{h} - C_f z_1}. \quad (45)$$

Rearrangement of the equation above results in the surface in-plane strain characteristic to be accurately modeled by

$$\varepsilon_S = \frac{A}{W_{\text{MDFZ}}} \ln\left(\frac{W_{\text{MDFZ}}}{b}\right) + \frac{A}{h} - C_f z_1. \quad (46)$$

The sum of the second and third terms yields a small contribution to the equation, since the boundary for the interfacial misfit dislocation free zone z_1 is very small in these structures, however, its value could be found by a similar approach where

$$\int_0^{z_1} \varepsilon(z) dz = \frac{E_d}{2b'Y} = \int_0^{z_1} C_f z dz = A \left[\ln\left(\frac{h-z_1}{b}\right) + 1 \right]. \quad (47)$$

Solving, the expression above results in transcendental expression similar to the Matthews and Blakeslee critical layer thickness equation as is applicable to linearly-graded layers,

$$z_1 = \sqrt{\frac{2A}{C_f} \left[\ln\left(\frac{h-z_1}{b}\right) + 1 \right]}. \quad (48)$$

Therefore, Eq. 46 is modified accordingly to

$$\varepsilon_S = \frac{A}{W_{\text{MDFZ}}} \ln\left(\frac{W_{\text{MDFZ}}}{b}\right) + \frac{A}{h} - \sqrt{2AC_f \left[\ln\left(\frac{h-z_1}{b}\right) + 1 \right]}. \quad (49)$$

If we make the exact simplifying assumptions as the previous models, the expressions given in Eqs. 45 and 46 reduce to the ones provided by Tersoff.

S-Graded Epitaxial Layers

The advantage of the electrical circuit model, in addition to providing an intuitive understanding of equilibrium lattice relaxation by analogy, is that it is the development of an analytical model for the strain and dislocation density in any compositionally-graded layer. As a specific example, we consider the nonlinear S-graded epitaxial layer investigated by Kujofsa et al.⁹ and Xhurxhi et al.²⁴ The lattice mismatch profile in the S-graded metamorphic buffer layer (SG-MBL) is designed to be a normal cumulative distribution function, given by

$$f(z) = \begin{cases} \frac{f_h - f_0}{2} \left[-\operatorname{erf}\left(\frac{\mu - z}{\sigma\sqrt{2}}\right) + \operatorname{erf}\left(\frac{\mu}{\sigma\sqrt{2}}\right) \right], & z < \mu; \\ \frac{f_h - f_0}{2}, & z = \mu, \\ \frac{f_h - f_0}{2} \left[\operatorname{erf}\left(\frac{z - \mu}{\sigma\sqrt{2}}\right) + \operatorname{erf}\left(\frac{\mu}{\sigma\sqrt{2}}\right) \right], & z > \mu, \end{cases} \quad (50)$$

where μ is the “mean parameter,” σ is the “standard deviation parameter,” f_0 and f_h are the respective values of lattice mismatch at the interface and the surface of the SG-MBL with thickness h . Kujofsa et al.⁹ and Xhurxhi et al.²⁴ developed approximate models for the in-plane strain distribution; however, the residual strain in the dislocated region was modeled to within 10% of the actual value. Figure 8 illustrated the lattice mismatch profile for 100-nm-thick $\text{In}_x\text{Ga}_{1-x}\text{As}$ layer on Ga (001) which varies from zero (corresponding to zero indium mole fraction) at the substrate interface to $f_h = -0.71\%$ at the surface (corresponding to 10% indium mole fraction). The mean parameter was fixed at half of the epitaxial layer thickness $\mu = 50$ nm, and the standard deviation parameter was $\sigma = 10$ nm. The results of Fig. 8 show excellent agreement in the residual strain distributions, as determined by both the numerical results and the electrical circuit model.

CONCLUSION

We have developed an electrical circuit model to study equilibrium lattice relaxation in multilayered and compositionally-graded heterostructures. In this approach, each sublayer of an epitaxial structure is modeled by analogy to an electrical subcircuit utilizing an independent voltage source, an ideal diode, a resistor and an independent current source. Multilayered or graded semiconductor structures may be modeled by stacking the appropriate number of these building blocks, after which the numerical values of the node voltages in the circuit correspond to the equilibrium strains in the sublayers of the semiconductor structure. Use of this electric circuit analogy allows the modeling of semiconductor strained-layer structures by readily available circuit simulators, and makes it possible to translate the intuitive understanding of circuits to heteroepitaxial devices. Furthermore, the model may be extended to continuously-graded layers by considering the limit as the individual sublayer thicknesses are diminished to zero. This extension allows the development of analytical expressions for the strain, misfit

dislocation density, and critical layer thickness for a continuously-graded layer having an arbitrary profile. It is similar to the transition from circuit theory, using lumped circuit elements, to electromagnetics, using distributed electrical quantities. We show this development using first principles, but, in a more general sense, Maxwell’s equations of electromagnetics could be applied and this will be considered in a future publication.

REFERENCES

1. K. Streubel, N. Linder, R. Wirth, and A. Jaeger, *IEEE J. Sel. Top. Quant. Electron.* 8, 321 (2002).
2. O. Kwon, J. Boeckl, M.L. Lee, A.J. Pitera, E.A. Fitzgerald, and S.A. Ringel, *J. Appl. Phys.* 97, 034504 (2005).
3. P. Lever, H.H. Tan, and C. Jagadish, *J. Appl. Phys.* 95, 5710 (2004).
4. D. Bimberga, M. Grundmanna, F. Heinrichsdorff, N.N. Ledentsov, V.M. Ustinov, A.E. Zhukov, A.R. Kovsh, M.V. Maximov, Y.M. Shernyakov, B.V. Volovik, A.F. Tsatsul’nikov, P.S. Kop’ev, and Z.I. Alferov, *Thin Solid Films* 367, 235 (2000).
5. D.E. Grider, S.E. Swirhun, D.H. Narum, A.I. Akinwande, T.E. Nohava, W.R. Stuart, P. Joslyn, and K.C. Hsieh, *J. Vac. Sci. Technol. B* 8, 301 (1990).
6. S. Mendach, C.M. Hu, Ch. Heyn, S. Schnull, H.P. Oepen, R. Anton, and W. Hansen, *Physica E* 13, 1204 (2002).
7. B. Bertoli, E.N. Suarez, J.E. Ayers, and F.C. Jain, *J. Appl. Phys.* 106, 073519 (2009).
8. T. Kujofsa and J.E. Ayers, *J. Vac. Sci. Technol. B* 32, 031205 (2014).
9. T. Kujofsa, A. Antony, S. Xhurxhi, F. Obst, D. Sidoti, B. Bertoli, S. Cheruku, J.P. Correa, P.B. Rago, E.N. Suarez, F.C. Jain, and J.E. Ayers, *J. Electron. Mater.* 42, 3408 (2013).
10. T. Kujofsa and J.E. Ayers, *J. Electron. Mater.* 45, 2831 (2016).
11. T. Kujofsa and J.E. Ayers, *J. Electron. Mater.* 43, 2993 (2014).
12. J.W. Matthews and A.E. Blakeslee, *J. Cryst. Growth* 27, 118 (1974).
13. J. Tersoff, *Appl. Phys. Lett.* 62, 693 (1993).
14. J. Tersoff, *Appl. Phys. Lett.* 64, 2748 (1994).
15. J.W. Matthews, *Epitaxial Growth, Part B* (New York: Academic, 1975).
16. V. Bush, *J. Franklin Inst.* 217, 289 (1934).
17. S. Whitehead, *J. Sci. Instrum.* 21, 73 (1944).
18. R.B. Stambaugh, *Ind. Eng. Chem.* 44, 1590 (1952).
19. S. Frieberg, *Exp. Mech.* 2, 24 (1962).
20. R. Olsson and M. Bath, *Phys. Earth Planet Inter.* 10, 1 (1975).
21. T. Kujofsa and J.E. Ayers, *Semicond. Sci. Technol.* 31, 115014 (2016).
22. J.E. Ayers, *Semicond. Sci. Technol.* 23, 045018 (2008).
23. D. Sidoti, S. Xhurxhi, T. Kujofsa, S. Cheruku, J.P. Correa, B. Bertoli, P.B. Rago, E.N. Suarez, F.C. Jain, and J.E. Ayers, *J. Appl. Phys.* 109, 023510 (2011).
24. S. Xhurxhi, F. Obst, D. Sidoti, B. Bertoli, T. Kujofsa, S. Cheruku, J.P. Correa, P.B. Rago, E.N. Suarez, F.C. Jain, and J.E. Ayers, *J. Electron. Mater.* 40, 2348 (2011).
25. J.E. Ayers, T. Kujofsa, P.B. Rago, and J.E. Raphael, *Heteroepitaxy of Semiconductors: Theory Growth and Characterization*, 2nd ed. (Boca Raton: CRC Press, 2016).
26. E.A. Fitzgerald, Y.-H. Xie, D. Monroe, P.J. Silverman, J.M. Kuo, A.R. Kortan, F.A. Thiel, and B.E. Weir, *J. Vac. Sci. Technol. B* 10, 1807 (1992).
27. D.J. Dunstan, *Phil. Mag.* A73, 1323 (1996).
28. F. Romanato, E. Napolitani, A. Carnera, A.V. Drigo, L. Lazzarini, G. Salviati, C. Ferrari, A. Bosacchi, and S. Franchi, *J. Appl. Phys.* 86, 4748 (1999).